ARTICLES SCIENCE CHINA Materials

mater.scichina.com link.springer.com

Published online 20 February 2017 | doi: 10.1007/s40843-016-9005-9
Sci China Mater 2017, 60(3): 258–268

Graphene oxide-Fe_3O_4 nanocomposites as high-performance antifungal agents against *Plasmopara viticola*

Xiuping Wang[1], Aijun Cai[1], Xiaolei Wen[1], Dapeng Jing[1], Huixia Qi[1] and Hong Yuan[2*]

ABSTRACT ***Plasmopara viticola*, a causal agent of grapevine downy mildew, is a widely distributed pathogen, which can cause destructive disease in field-grown grapevines. Although fungicides are used to treat the disease, fungicide-resistant strains have been emerging. In this study, we developed graphene oxide (GO)-Fe_3O_4 nanocomposites, which could effectively repress the germination of sporangia and inhibit the development of downy mildew. 50 μg mL^{-1} GO-Fe_3O_4 showed excellent protective and fungicidal activities. 250 μg mL^{-1} GO-Fe_3O_4 on grapevine leaves in the field could significantly decrease the severity of downy mildew, suggesting its potent curative effect. Moreover, GO-Fe_3O_4 had no significant toxic effects on grapevine plants even at the concentration twice that of the highest dosage (1000 μg mL^{-1}) used in this study. Our work suggested that GO-Fe_3O_4 would offer an important opportunity to develop new approach for controlling plant diseases.**

Keywords: GO-Fe_3O_4, disease management, antifungal agents, grapevine downy mildew

INTRODUCTION

Grapevine (*Vitisvinifera*) is one of the major fruit crops worldwide [1]. However, grapevine downy mildew, one of the most destructive diseases caused by *Plasmopara viticola* (*P. viticola*) [2], can lead to significant reduction (by 20%–30%) of yield [3–5]. Disease management has been one of the major tasks for viticulture after the infection of the plant by downy mildew [6]. To effectively control the disease and avoid substantial yield loss, chemical fungicide is the optimal choice [4]. However, the intensive use of synthetic fungicides becomes more and more restricted due to their negative impacts on the environment and humans [7]. In addition, pesticide residues affect the natural yeast communities and aroma of wine, which are important factors in wine production [8,9]. Thus, it is highly desirable to develop alternative strategies to reduce the use of conventional chemical inputs for the protection against diseases in vineyard.

Graphene possesses interesting physical and chemical properties, and has a wide range of technological applications in recent years [10–12]. In particular, great efforts have been devoted to exploring graphene oxide (GO) as novel antimicrobial agents with a severe cytotoxic effect on bacteria [13–16], fungi [17,18], and plant pathogens [19,20]. GO and other graphite-based materials can inhibit the growth of gram-negative and gram-positive bacteria such as methicillin-resistant *Staphylococcus aureus*, *Staphylococcus aureus* and *Escherichia coli* [13,14]. Our previous study demonstrated that GO had inhibitory effects against plant pathogenic fungi (*Fusarium graminearum* and *Fusarium poae*) and bacteria (*Ralstonia solanacearum* and *Xanthomonas oryzae pv. Oryzae*) [18,19]. However, the excellent bactericidal activity of GO reported was dependent on its use at relatively high doses, which would raise the cost of production as well as causing potential pollution to the environment.

Recently, considerable progress has been made on the interaction between inorganic nanomaterials (NMs) and biomolecules (such as DNA, protein and amino acids), which provides an excellent platform for the application of inorganic NMs [21–26]. Several inorganic NMs were used as antimicrobial agents for the protection of crops and animals from pathogen infection [27–30]. Among them, iron

[1] College of Life Science and Technology, Hebei Normal University of Science and Technology, Qinhuangdao 066004, China
[2] Key Laboratory of Pesticide and Chemical Biology of Ministry of Education, Institute of Environmental Chemistry, College of Chemistry, Central China Normal University, Wuhan 430079, China
* Corresponding author (email: yuanhong@mail.ccnu.edu.cn)

oxide nanoparticles (NPs) are effective biocides against a variety of pathogens [31]. However, the agglomeration of bare iron oxide NPs resulted in the loss of active surface area and weakened its antibacterial activity. So researchers focused on enhancing the antibacterial activity of iron oxide. Recent reports demonstrated that the combination of GO with NPs (particularly metal oxide NPs) offered a number of unique physicochemical properties, which were highly desirable and markedly advantageous for bio-applications [32]. Therefore, integrating Fe_3O_4 NPs and GO into GO-Fe_3O_4 nanocomposites could be a promising solution to control plant diseases.

This study was aimed to investigate the apparent antifungal activity of GO-Fe_3O_4 nanocomposites against *P. viticola*, a kind of strictly biotrophic pathogenic fungi. The protective, fungicidal and curative activities of GO-Fe_3O_4 were evaluated *in vivo*. The antifungal activity of GO-Fe_3O_4 was compared with that of Fe_3O_4 or GO alone. Moreover, the phytotoxicity of GO-Fe_3O_4 in nature was also studied, which was a prerequisite for its application as antifungal agents in plant protection.

MATERIALS AND METHODS

Materials

All chemicals were analytical grade reagents, and were used as received without further purification. Graphite was purchased from Qingdao Tianhe Graphite Co. Ltd., with an average particle diameter of 4 mm (99.95% purity). Polyvinylpyrrolidone (PVP), 3-aminopropyltrimethoxysilane (APS) and 1-ethyl-3-(3-dimethyamino-propyl) carbodiimide (EDC) were purchased from Sigma-Aldrich Co. (USA). All other reagents were obtained from Tianjin No. 3 Chemical Plant.

Characterization

A transmission electron microscope (TEM, FEI, TECNAI-20) was used to characterize the size and morphology of GO, Fe_3O_4 and GO-Fe_3O_4. Particle size distributions were measured using a Zetasizer Nano ZS90 dynamic light scattering (DLS) system (Malvern, England). Its crystal structure was characterized by X-ray diffraction measurements (XRD, Bruker D8-ADVANCE, Cu Kα radiation, Germany).

Preparation of Fe_3O_4 NPs

Fe_3O_4 NPs were synthesized by a modified procedure as previously reported [33]. Briefly, 2 mmol $FeSO_4{\cdot}7H_2O$ and 1.0 g PVP were dissolved in 80 mL deionized (DI) water with magnetic stirring. The solution was then heated rapidly to 90°C, followed by the addition of 10 mL NaOH aqueous solution (1 mol L^{-1}). After being stirred for 60 min, the solution was cooled to room temperature. The products were collected by centrifugation, and then washed thoroughly with water. After Fe_3O_4 was dried under vacuum at room temperature, 100 mg samples were sonicated for 40 min in 150 mL solution of DI water-ethanol (1:2, *v*/*v*). Then, the solution was stirred at 40°C for 8 h with the addition of 1 mL APS. Lastly, the obtained Fe_3O_4 was washed several times with water and ethanol, and then dried in vacuum overnight [34].

Preparation of GO

The commercially available graphite powder was oxidized and exfoliated to GO following the method previously described by our group [18].

Preparation of GO-Fe_3O_4 nanocomposites

According to the report of Li's group [34], GO (80 mg) and Fe_3O_4 (20 mg) were dispersed in 100 mL ultrapure water. The mixture was ultrasonicated for 60 min, and then stirred at 80°C for 24 h after adding EDC (20 mg). The black product was washed thoroughly with DI water, and dried at 50°C in a vacuum oven.

Plant materials and growth conditions

Grapevine leaves of Cabernet Sauvignon cultivar were used to study the apparent antifungal effect of GO-Fe_3O_4 on downy mildew in laboratory. Grapevine plants (*Vitisvinifera L.* cv. Cabernet Sauvignon) were propagated from wood cuttings in a greenhouse. All tests were performed with fully expanded grapevine leaves from the fourth to sixth leaf positions from the shoot tip on foliar discs [4].

An isolate of *P. viticola* was obtained from a natural field infection in a vineyard in Qinhuangdao region, China, and maintained on reinfected plants grown in a growth chamber at a temperature of 24 and 18°C (day and night, respectively) with a photoperiod of 16 h of light and at a relative humidity (RH) of 70 ± 10% [5]. Inoculum of *P. viticola* sporangia was prepared by washing the leaves bearing sporulating lesions with cold (5°C) distilled water and adjusted to a concentration of 1×10^5 sporangia mL^{-1} by counting with a haemocytometer [35].

Protective effect of GO-Fe_3O_4 against *P. viticola*

Leaves obtained from the same position on the shoot tip (fourth to sixth unfolded leaf) were surface-sterilized with 70% (*v*/*v*) ethanol, and subsequently rinsed with DI water [36]. Leaf discs of 0.9 cm diameter were punched from different acclimatized plants using a cork-borer and placed

upside-down in Petri dishes containing suspensions of different concentrations of GO, Fe_3O_4, GO-Fe_3O_4 (without any surfactant). Controlled leaf discs were treated with distilled water. One day later, each disc was inoculated by spraying of a fresh sporangial suspension (1×10^5 sporangia mL^{-1}) using a manual sprayer device. After that, they were incubated in a growth chamber at 20°C and 70% RH and under a 16 h light/8 h dark photo period till artificial inoculation. The experiments were repeated twice with four Petri dishes for each treatment batch and 24 leaf discs were used for each Petri dish [5]. Quantitative symptoms of infection such as disease incidence and disease index, were visually analyzed as independent parameters 7 d after inoculation. The disease incidence (the total percentage of leaves with symptoms in the total number of leaves) and disease severity (the percentage of the leaf disc area exhibiting symptoms of sporulation) were assessed as described by Boso and Kassemeyer [37].

The control efficacy of GO, Fe_3O_4, GO-Fe_3O_4 was calculated using the following formula:

$$\text{Control efficacy (\%)} = \left(1 - \frac{\text{disease index of treatment}}{\text{disease index of control}}\right) \times 100.$$

Fungicidal effect of GO-Fe_3O_4 against *P. viticola*

The direct effect of GO-Fe_3O_4 on *P. viticola* sporangia germination *in vitro* was performed as previously described by Perazzoli [38]. In brief, 80 μL suspension of spores was mixed with 80 μL of GO, Fe_3O_4, GO-Fe_3O_4 in the tubes at its final concentration of 50, 100, 250 and 500 μg mL^{-1}, respectively. Control samples containing 80 μL suspensions of spores were mixed with 80 μL DI water. 30 μL mixture, containing different concentration of GO, Fe_3O_4, GO-Fe_3O_4, was transferred to a concave slide. After further incubating for 8 h in darkness at 20°C, the percentages of the germinated sporangia (emptied) were counted under a light microscope in four replicates (50 sporangia per treatment). Sporangia germination rate (%) was calculated as (the number of germinated sporangia)/(the total number of sporangia).

The curative effect of GO-Fe_3O_4 against *P. viticola*

To assess the curative activity of GO-Fe_3O_4 on grapevine plants, grapevine leaves naturally infected with the downy mildew pathogen, were sprayed with the solution of 250 μg mL^{-1} GO-Fe_3O_4. After treating with GO-Fe_3O_4 for three or seven days, the disease severity was assessed, and the control efficiency was calculated.

The phytotoxicity of GO-Fe_3O_4 on grapevine plants

To assess the phytotoxicity of GO-Fe_3O_4 on grapevine plants, acclimatized plants were sprayed with 1000 μg mL^{-1} GO-Fe_3O_4. After seven days, the phytotoxicity of GO-Fe_3O_4 were recorded.

RESULTS AND DISCUSSION

Characterization of GO-Fe_3O_4 nanocomposites

Typical XRD patterns of GO, Fe_3O_4, and GO-Fe_3O_4 are presented in Fig. S1. GO shows a strong peak at $2\theta = 10.3°$, which is a feature diffraction peak of exfoliated GO [39]. According to the JCPDS file No. 65-3107, the diffraction peaks at $2\theta = 30.1°$, 35.6°, 43.2°, 53.8°, 57.5° and 62.9°, could be attributed to (220), (311), (400), (511), and (440) crystal planes of cubic Fe_3O_4 [33]. For GO-Fe_3O_4, the characteristic peaks of Fe_3O_4 are observed clearly. However, the characteristic diffraction peaks of GO become weakened or even disappeared in GO-Fe_3O_4 nanocomposites, because the regular stacks of GO were exfoliated during the ultrasonic treatment, which correlates well with the previous studies [40,41].

Raman spectroscopy is a powerful tool for the characterization of carbon NMs, which can provide the information about the structural changes [32]. The main features in the Raman spectra of graphene-like materials were their G and D bands (1583 and 1340 cm^{-1}), and the intensity ratio of D and G band (I_D/I_G) was assigned to its lower defects/disorders. As shown in Fig. S2, the I_D/I_G of GO-Fe_3O_4 increases to 1.06 compared with that of GO (0.99), indicating the presence of localized sp^3 defects within sp^2 carbon network. Moreover, it is clear that G band of GO-Fe_3O_4 appears at 1591 cm^{-1}, which is down shifted by 8 cm^{-1}. The Raman shift of G band for GO-Fe_3O_4 provides a strong evidence about the strong interaction between GO and Fe_3O_4. Furthermore, D band of GO-Fe_3O_4 becomes lower and broader with respect to pristine GO, suggesting the increase of its disorder [42,43].

The morphologies of Fe_3O_4, GO and GO-Fe_3O_4 were characterized using TEM. Fig. 1a shows the TEM image of pure Fe_3O_4 NPs, which possess an arrow particle size distribution ranging from 30 to 36 nm. The GO sheets were thin, transparent and smooth with small wrinkles (Fig. 1b). It is shown in Fig. 1c that a large amount of Fe_3O_4 NPs are anchored onto the surfaces of GO substrates. The interaction between GO and Fe_3O_4 NPs is resulted from their surface properties. There are lots of carboxylic acid groups on the surface of GO that obtained by oxidization and exfoliation from graphite powder [18]. The Fe_3O_4 NPs were modified by APS to introduce amino groups on their

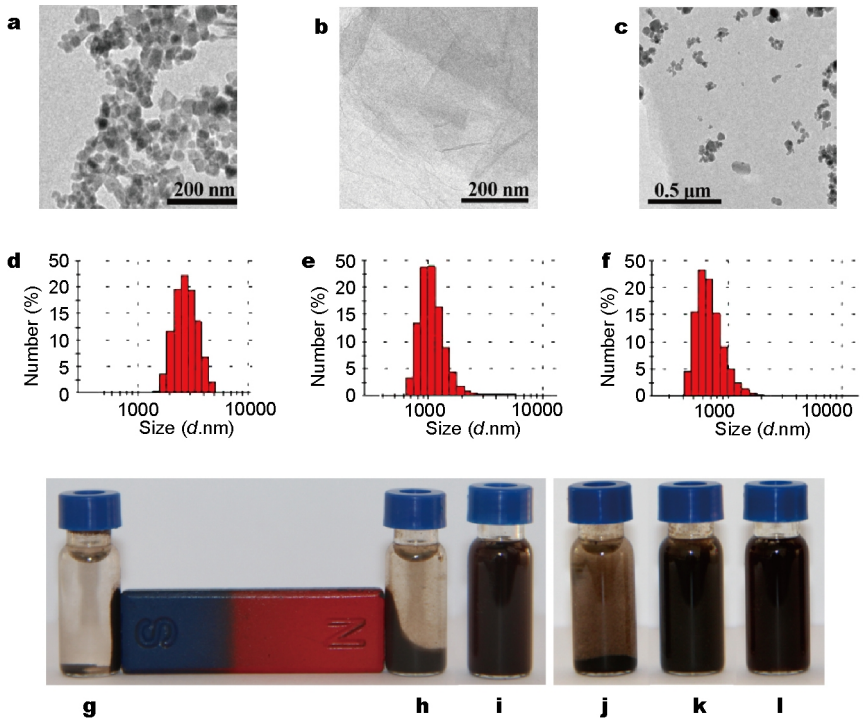

Figure 1 TEM images of Fe_3O_4 (a), GO (b) and GO-Fe_3O_4 (c). DLS size distributions of Fe_3O_4 (d), GO (e) and GO-Fe_3O_4 (f) in water after 30 min sonication. Photographic images of Fe_3O_4 (g), GO-Fe_3O_4 (h) and GO (i). The dispersity and stability of Fe_3O_4 (j), GO-Fe_3O_4 (k), and GO (l) after being stored for seven days.

surface [40]. So the conjugation reactions occurred between the amino group of Fe_3O_4 and the carboxylic group of GO in the presence of cross-linker EDC. The dispersity of Fe_3O_4, GO and GO-Fe_3O_4 was further confirmed by DLS. Fig. 1d shows that Fe_3O_4 formed large aggregates in water. However, the effective diameters of GO-Fe_3O_4 were smaller than those of GO and Fe_3O_4. This result shows that the dispersity of Fe_3O_4 was better after being immobilized onto GO sheets. The magnetic manipulation of Fe_3O_4 and GO-Fe_3O_4 were tested (Fig. 1g, h). When Fe_3O_4 and GO-Fe_3O_4 dispersed in water were placed in an external magnetic field, the efficient magnetic separation was observed within several minutes. After removing the magnet, GO-Fe_3O_4 could be uniformly re-dispersed in water and form a stable suspension. We also observed that Fe_3O_4 could not be dispersed in water, but GO and GO-Fe_3O_4 could be dispersed to form a homogeneous black solution, which was stable after seven days (Fig. 1j, k). Such good dispersity of GO-Fe_3O_4 in aqueous media compared with that of Fe_3O_4 NPs alone, is serviceable as the antifungal agents in plant protection.

Protective activity of GO-Fe_3O_4 against *P. viticola*

Vitisvinifera L. cv. Cabernet Sauvignon leaf discs were pretreated with Fe_3O_4, GO and GO-Fe_3O_4 at different concentrations for one day, and then inoculated with a *P. viticola* sporangium suspension. White sporulation symptoms of *P. viticola* could be observed by naked eyes at 5 days post-inoculation (dpi). 83.2% of the leaf discs were covered with *P. viticola* sporulation symptoms in water-treated samples (Fig. 2a). In contrast, for samples pretreated with bare Fe_3O_4 and GO, the percentage of disease incidence varied from 54.68% to 13.89% and 44.89% to 12.22%, respectively. Particularly, after treated by GO-Fe_3O_4, the percentage of disease incidence varied from 25.56% to 8.89%. These data showed that the downy mildew development was significantly inhibited by Fe_3O_4, GO and GO-Fe_3O_4 in a dose-dependent manner.

Fig. 2b shows the effects of Fe_3O_4, GO and GO-Fe_3O_4 on the disease severity of *P. viticola*. The percentage of leaf area (abaxial surfaces) covered by sporangiophores and sporangia was found to be significantly decreased after being treated with Fe_3O_4, GO and GO-Fe_3O_4. In water-treated leaf discs, 46.7% of the area was covered by *P. viticola* sporulation. In samples pretreated with Fe_3O_4 and GO, the area covered by *P. viticola* sporulation was reduced to 38.45%–24.02%, and 34.91%–13.89%, respectively. Particularly, the disease severity significantly dec-

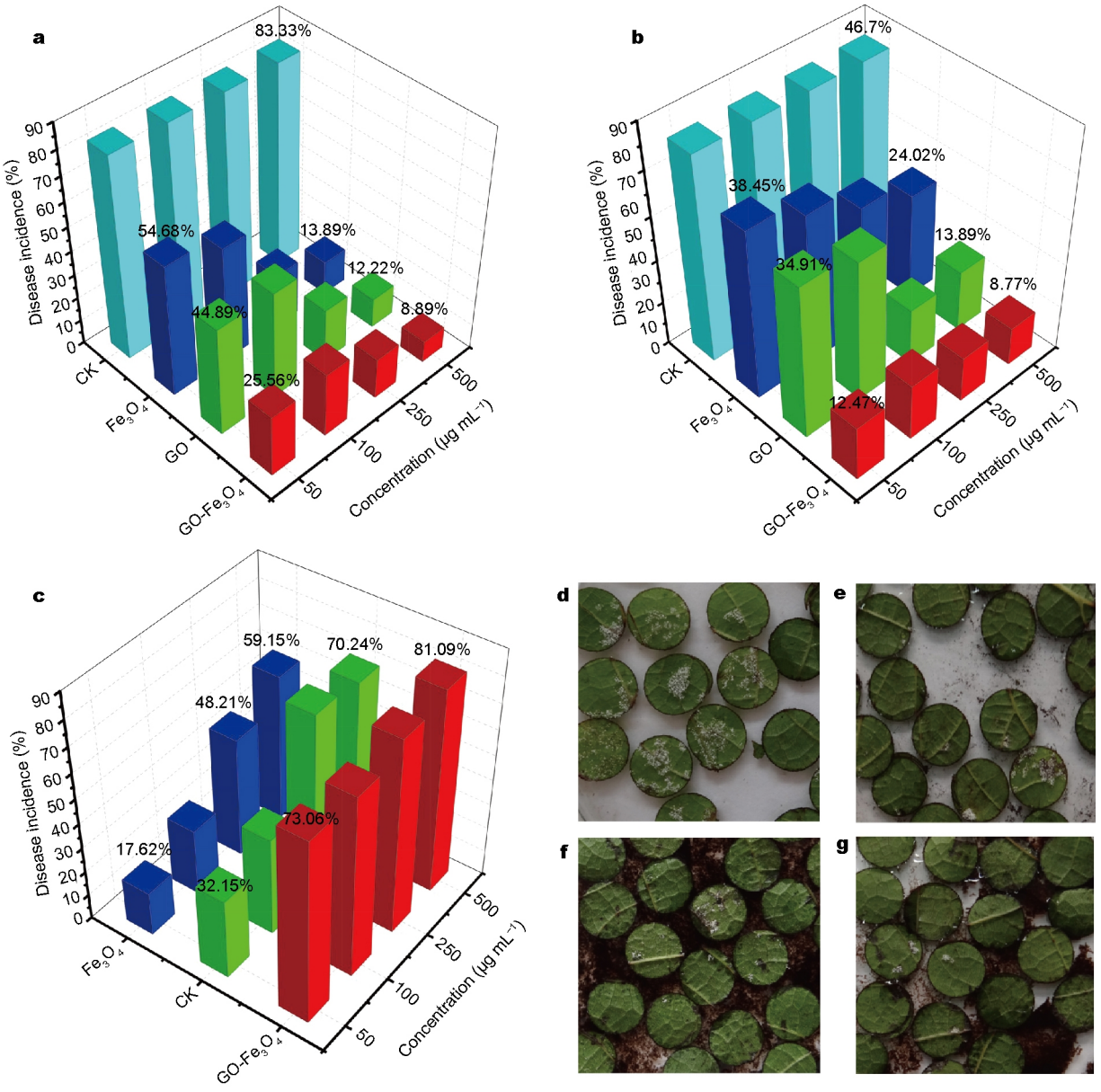

Figure 2 Protective activities (a–c) and images (d–g) of GO, GO-Fe_3O_4 and Fe_3O_4 on leaf discs of grapevines against *P. vticola*. Effects of GO, GO-Fe_3O_4 and Fe_3O_4 on disease incidence (percentage of infected leaves) of downy mildew (a), the disease index (percentage of leaf disc area exhibiting symptoms of sporulation) of downy mildew (b), and controlling downy mildew (c). Images of leaf discs treated with DI water (d), Fe_3O_4 (e), GO (f), and GO-Fe_3O_4 (g) at 5 dpi at with concentration of 250 μg mL^{-1}.

reased to 12.47%–8.77% after treated by GO-Fe_3O_4. These data show that Fe_3O_4, GO and GO-Fe_3O_4 treatments could significantly inhibit downy mildew development.

Finally, the control efficacy of GO, Fe_3O_4 and GO-Fe_3O_4 on grape downy mildew development was compared on leaf discs. As shown in Fig. 2c, GO, Fe_3O_4, and GO-Fe_3O_4 are highly effective in suppressing downy mildew development. The control efficacy of GO nanosheets and Fe_3O_4 NPs was 17.62%, and 32.15% at the concentration of 50 μg mL^{-1}, respectively. When the concentration increased to 500 μg mL^{-1}, the control efficacy increased to 59.15% and 70.24%, respectively. However, GO-Fe_3O_4 had the highest efficacy in inhibiting fungal growth. Even at the lowest concentration (50 μg mL^{-1}), GO-Fe_3O_4 could control >73.6% of *P. viticola*. To achieve similar control efficacy, the dosage of GO should be 500 μg mL^{-1}, which is 10 times that of GO-Fe_3O_4. These results clearly indicated that GO-Fe_3O_4 even at a very low concentration was more

effective than GO and Fe_3O_4 in protecting the plant against downy mildew. In actual production, pathogen invasion of the plants could be prevented by spraying GO-Fe_3O_4 on the surface of plants before pathogen infection.

Fig. 2d–g show the corresponding photomicrograph of leaf discs after treating with 250 μg mL^{-1} Fe_3O_4, GO, or GO-Fe_3O_4, which visually confirms that Fe_3O_4 (Fig. 2e), GO (Fig. 2f) and GO-Fe_3O_4 (Fig. 2g) could effectively restrain the percentage of leaves with symptoms. Especially, for GO-Fe_3O_4 treatment, a very limited number and area of leaf discs were found to exhibit symptoms of sporulation.

Inhibitory activity of GO-Fe_3O_4 on germination of sporangia

With favorable weather, sporangia would attach to the host surface, and release zoospores that establish new secondary infections. However, if the germination of sporangia is inhibited or stopped, the zoospores cannot be released and initiate the new infection cycle [44]. Therefore, it is necessary to investigate the inhibitory effects of these materials on the germination of sporangia. The bare Fe_3O_4 NPs at the concentrations of 50, 100, 250 and 500 μg mL^{-1} could inhibit the germination of sporangia (Fig. 3). The germination rate of sporangia was merely more than 46.6% at the highest concentration. Bare GO showed a stronger antifungal activity than bare Fe_3O_4. At the highest concentration of GO, the germination rate of sporangia was 22.8%. GO-Fe_3O_4 showed a higher efficacy in inhibiting the germination of sporangia. Even at the lowest concentration (50 μg mL^{-1}), GO-Fe_3O_4 could inhibit >81.25% of sporangium germination. These results showed that GO-Fe_3O_4 had the strongest activity in inhibiting the germination of sporangia.

Fig. 4 displays the representative microscopic images of sporangium germination after being treated with GO, Fe_3O_4 and GO-Fe_3O_4. The germinated sporangia were empty because the zoospores had been released (Fig. 4a). However, in the sporangia treated by GO, Fe_3O_4 and GO-Fe_3O_4, the sporangia were full of zoospores. Especially, for those treated by GO-Fe_3O_4, nearly 85% of the sporangia were ungerminated, confirming that GO-Fe_3O_4 could effectively restrain the sporangium germination of *P. vticola*. Such inhibitory effect on sporangium germination indicated its direct toxic effect against the pathogen [5].

Our previous work showed that GO could significantly inhibit the spore germination of *F. graminearum* and *F. poae* [18,19]. Water channel blockage of the spore caused by surface-adsorbed GO could be one main factor for the inhibition of spore germination [18]. In the present study, the same phenomenon was observed in the sporangia treated by GO, Fe_3O_4 and GO-Fe_3O_4. As shown in Fig. 4, a few clusters of GO, Fe_3O_4 and GO-Fe_3O_4 could interact with sporangia. Therefore, we also believe that water channel blockage of the sporangia caused by surface-adsorbed NMs plays an important role in the inhibition of sporangium germination.

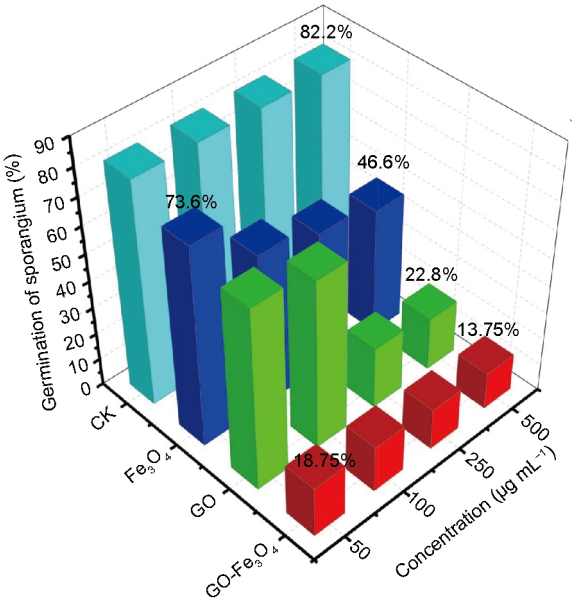

Figure 3 Inhibitory activity of GO, Fe_3O_4 and GO-Fe_3O_4 on the germination of sporangia.

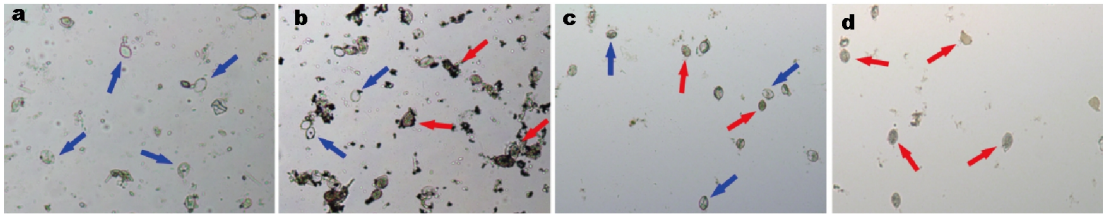

Figure 4 Microscopic images of sporangia untreated (a), and treated with Fe_3O_4 (b), GO (c), and GO-Fe_3O_4 (d) at a concentration of 50 μg mL^{-1}. Blue arrows indicate the germinated sporangia; and red arrows indicate the ungerminated sporangia.

Curative activity of GO-Fe_3O_4 against downy mildew

After the leaves were infected by downy mildew, the application of GO, Fe_3O_4, and GO-Fe_3O_4 at 250 μg mL^{-1} on grape leaves under field conditions significantly decreased the severity of downy mildew disease as compared with the control experiment. As shown in Fig. 5, the disease severity of the control was 2.4% at the beginning of the experiment. Seven days later, the disease severity was 35.28%. The disease severity before the treatment with Fe_3O_4, GO and GO-Fe_3O_4 was 2.86%, 2.67% and 1.83%, respectively. After seven days treatment, the disease severity of leaves was increased to 32.43%, 17.37% and 12.42%, respectively. The control efficacy of Fe_3O_4, GO and GO-Fe_3O_4 was 36.65%, 51.24% and 65.08%, respectively. These results show that more effective and durable inhibitory activity towards downy mildew was observed at three and seven days after treated with GO, Fe_3O_4 and GO-Fe_3O_4 (Fig. 6). After seven days, the control efficacy of GO-Fe_3O_4 was still more than 65%, which was much higher than those of GO and Fe_3O_4. Fig. 6 shows the corresponding photograph of severity of downy mildew treated by 250 μg mL^{-1} GO, Fe_3O_4 and GO-Fe_3O_4. It was visually confirms that GO, Fe_3O_4, GO-Fe_3O_4 could effectively inhibit the development of downy mildew. Especially, GO-Fe_3O_4 could remarkably decrease the infection of downy mildew. The curative activity of GO-Fe_3O_4 was obviously related to their inhibition of sporangium germination. Sporangium germination was first inhibited, and then the spores could not be released and germinate to form hyphae, thereby resulting in inhibited development of downy mildew.

The above results indicate that GO-Fe_3O_4 displayed higher protective, fungicidal and curative activity than bare Fe_3O_4 and GO. We thus proposed that GO-Fe_3O_4 had the synergistic effect between Fe_3O_4 and GO. It is believed that that the dispersity of materials should strongly influence their interaction with leaf or sporangia. GO-Fe_3O_4 with a higher dispersity was more protective to leaf and could better inhibit the germination of sporangia than Fe_3O_4 with a lower dispersity, which had more opportunities to interact with the leaf or sporangia. Similar phenomena had been previously observed on other NMs. For instance, GO

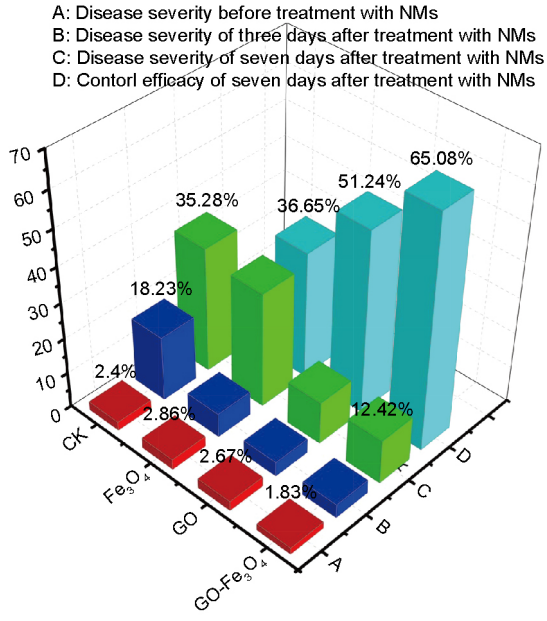

Figure 5 Disease severity and control efficacy of GO, Fe_3O_4, and GO-Fe_3O_4 on controlling downy mildew in field-grown grapevine at the concentrations of 0 and 250 μg mL^{-1}.

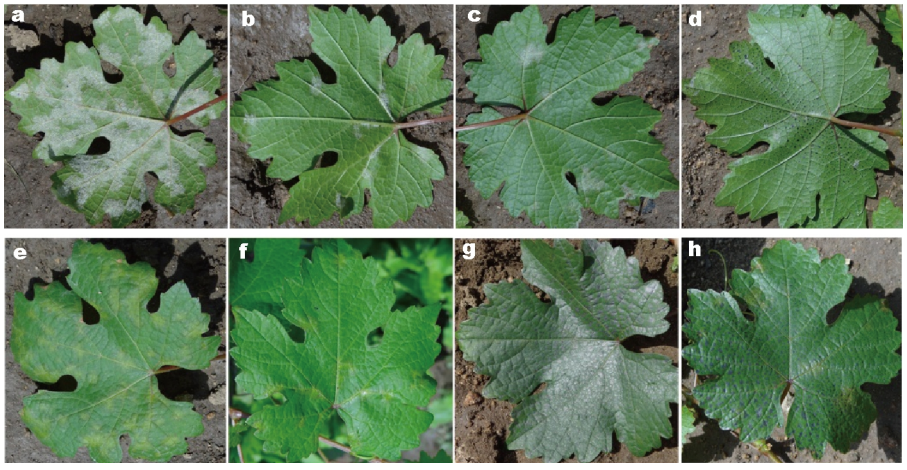

Figure 6 Grape plants treated without (a, e) and with Fe_3O_4 (b, f), GO (c, g), and GO-Fe_3O_4 (d, h) at 250 μg mL^{-1}. In the upper row are the images of the abaxial surfaces of leaves; in the lower row are the images of the adaxial surfaces of leaves.

could form stable dispersions, and therefore showed higher toxicity to various bacterial cells and fungi than reduced GO (rGO) aggregates [14,18,20]. Functioned carbon nanotubes (CNTs) displayed stronger toxicity compared with as-synthesized CNT aggregates [45]. Moreover, the differences in the dispersity of GO, Fe_3O_4 and GO-Fe_3O_4 would be responsible for their different stabilities and adsorption properties on leaves. It could also be seen from Fig. 6f–h that after spraying, GO and GO-Fe_3O_4 could adsorb on both the abaxial and adaxial surfaces of leaves, whereas no Fe_3O_4 was observed on both sides of grape leaves. Furthermore, smaller and more droplets were uniformly dispersed on GO-Fe_3O_4 treated leaves compared with on those GO-treated leaves. This was likely due to that the lower the dispersity was (e.g., Fe_3O_4), the larger droplets were formed when spraying, and then the easier it fell off. The higher the dispersity was, the smaller and more droplets there would be, and the better and stronger the stability and adsorption would be, thus resulting in more effectiveness in controlling the infection of downy mildew. Therefore, GO-Fe_3O_4 had the highest curative activity, followed by GO and Fe_3O_4.

One of the key outcomes of the study was the potent antifungal effects of GO-Fe_3O_4 at a very low concentration. At the concentration of 50 μg mL^{-1}, GO-Fe_3O_4 showed excellent protective and fungicidal ability. However, the curative activity of GO-Fe_3O_4 was lower than chemical fungicides (in general, the control efficacy of chemical fungicides was more than 70%). This phenomenon should be attributed to the additives in the pesticide formulations, which improve the ability of the pesticide to penetrate, target or protect the target organisms. Therefore, chemical fungicides appeared to be more effective in plant protection. The formulation of GO-Fe_3O_4 as active ingredients was needed in plant protection. In China, a large amount of synthetic chemical fungicides are applied annually on grapes. GO-Fe_3O_4 could be one of the most promising alternative strategies for managing grapevine downy mildew.

Interestingly, our results showed that the protective, fungicidal and curative activities of GO-Fe_3O_4 could be regulated in a time-dependent manner before or after infection of plants by downy mildew. We applied GO-Fe_3O_4 at least one day before pathogen inoculation, and GO-Fe_3O_4 showed excellent protective activity. However, after many hours of direct contact with the sporangia, GO-Fe_3O_4 inhibited the germination of spores, suggesting their strong and direct fungicidal activity. After the infection by downy mildew, GO-Fe_3O_4 on grape leaves significantly reduced the severity of downy mildew, suggesting their excellent curative activity. In real production, GO-Fe_3O_4 could be applied according to the actual progression of downy mildew. For example, in Qinhuangdao area, grape downy mildew usually occurred in late July. Thus, the leaves could be pre-treated by GO-Fe_3O_4 to protect plants from the attack of *P. viticola*. However, once downy mildew occurred, leaves could be treated directly by GO-Fe_3O_4 for controlling the development of the disease.

Phytotoxicity of GO-Fe_3O_4 on plants

In order to determine the phytotoxicity of Fe_3O_4, GO and GO-Fe_3O_4, the leaves of plants were treated with 1000 μg mL^{-1} for seven days in the vineyard. As shown in Fig. 7, the treated plant leaves did not exhibit cell death or any abnormalities. Additionally, it was difficult for GO to translocate between different tissues in plants [46]. Similarly, GO-Fe_3O_4 desorbed on the leaves was also difficult to be translocated to other parts of the plant, which could decrease the potential risk to the environment and human health. These results suggested its potential commercial-ization in the management of fungal diseases in vegetable and other crops worldwide.

CONCLUSION

In conclusion, our study showed the potent antifungal activity of GO-Fe_3O_4 towards *P. vticola*, a model plant pathogenic fungus, and their protective, fungicidal and curative activities. Optimal protective and fungicidal activities could be achieved with 50 μg mL^{-1} GO-Fe_3O_4. GO-Fe_3O_4 at 250 μg mL^{-1} could significantly depress the disease severity of downy mildew. High dosage of GO-Fe_3O_4 (1000 μg mL^{-1}) had no phytotoxic effect on plant leaves. The detailed molecular mechanisms of the activities of GO-Fe_3O_4 to-

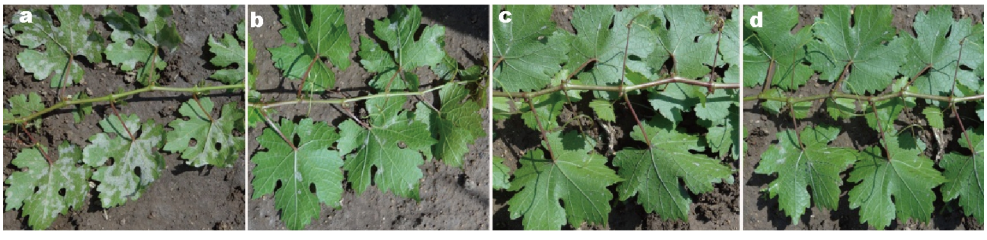

Figure 7 Treatment of grape plants without (a) and with Fe_3O_4 (b), GO (c), GO-Fe_3O_4 (d) at 1000 μg mL^{-1}.

wards *P. vticola* will be investigated in our future work. The safe application of GO-Fe_3O_4 at low concentrations would readily facilitate the environment-friendly disease management in vineyards.

Received 26 December 2016; accepted 24 January 2017; published online 20 February 2017

1 Banani H, Roatti B, Ezzahi B, *et al.* Characterization of resistance mechanisms activated by *Trichoderma harzianum* T39 and benzothiadiazole to downy mildew in different grapevine cultivars. Plant Pathol, 2014, 63: 334–343
2 Toffolatti SL, Venturini G, Maffi D, *et al.* Phenotypic and histochemical traits of the interaction between *Plasmopara viticola* and resistant or susceptible grapevine varieties. BMC Plant Biol, 2012, 12: 124–139
3 Pinto KMS, do Nascimento LC, de Souza Gomes EC, *et al.* Efficiency of resistance elicitors in the management of grapevine downy mildew *Plasmopara viticola*: epidemiological, biochemical and economic aspects. Eur J Plant Pathol, 2012, 134: 745–754
4 Alarcon AA, Lazazzara V, Cappellin L, *et al.* Emission of volatile sesquiterpenes and monoterpenes in grapevine genotypes following *Plasmopara viticola* inoculation *in vitro*. J Mass Spectrom, 2015, 50: 1013–1022
5 Boubakri H, Chong J, Poutaraud A, *et al.* Riboflavin (vitamin B2) induces defence responses and resistance to *Plasmopara viticola* in grapevine. Eur J Plant Pathol, 2013, 136: 837–855
6 Schwander F, Eibach R, Fechter I, *et al.* Rpv10: a new locus from the Asian Vitis gene pool for pyramiding downy mildew resistance loci in grapevine. Theor Appl Genet, 2012, 124: 163–176
7 Chen WJ, Delmotte F, Richard-Cervera S, *et al.* At least two origins of fungicide resistance in grapevine downy mildew populations. Appl Environ Microbiol, 2007, 73: 5162–5172
8 González Álvarez M, Noguerol-Pato R, González-Barreiro C, *et al.* Changes of the sensorial attributes of white wines with the application of new anti-mildew fungicides under critical agricultural practices. Food Chem, 2012, 130: 139–146
9 Milanović V, Comitini F, Ciani M. Grape berry yeast communities: influence of fungicide treatments. Int J Food Microbiol, 2013, 161: 240–246
10 Konwar A, Kalita S, Kotoky J, *et al.* Chitosan–iron oxide coated graphene oxide nanocomposite hydrogel: a robust and soft antimicrobial biofilm. ACS Appl Mater Interfaces, 2016, 8: 20625–20634
11 Yu L, Chen J, Liang Z, *et al.* Degradation of phenol using Fe_3O_4-GO nanocomposite as a heterogeneous photo-Fenton catalyst. Separation Purification Tech, 2016, 171: 80–87
12 Wan Z, Wang J. Ce-Fe-reduced graphene oxide nanocomposite as an efficient catalyst for sulfamethazine degradation in aqueous solution. Environ Sci Pollut Res, 2016, 23: 18542–18551
13 Akhavan O, Ghaderi E. Toxicity of graphene and graphene oxide nanowalls against bacteria. ACS Nano, 2010, 4: 5731–5736
14 Liu S, Zeng TH, Hofmann M, *et al.* Antibacterial activity of graphite, graphite oxide, graphene oxide, and reduced graphene oxide: membrane and oxidative stress. ACS Nano, 2011, 5: 6971–6980
15 Tu Y, Lv M, Xiu P, *et al.* Destructive extraction of phospholipids from *Escherichia coli* membranes by graphene nanosheets. Nat Nanotech, 2013, 8: 594–601
16 He J, Zhu X, Qi Z, *et al.* Killing dental pathogens using antibacterial graphene oxide. ACS Appl Mater Interfaces, 2015, 7: 5605–5611
17 Sawangphruk M, Srimuk P, Chiochan P, *et al.* Synthesis and antifungal activity of reduced graphene oxide nanosheets. Carbon, 2012, 50: 5156–5161
18 Wang X, Liu X, Chen J, *et al.* Evaluation and mechanism of antifungal effects of carbon nanomaterials in controlling plant fungal pathogen. Carbon, 2014, 68: 798–806
19 Chen J, Wang X, Han H. A new function of graphene oxide emerges: inactivating phytopathogenic bacterium *Xanthomonas oryzae pv. Oryzae*. J Nanopart Res, 2013, 15: 1658
20 Wang X, Liu X, Han H. Evaluation of antibacterial effects of carbon nanomaterials against copper-resistant *Ralstonia solanacearum*. Colloids Surf B-Biointerfaces, 2013, 103: 136–142
21 Liu W, Zhu Z, Deng K, *et al.* Gold nanorod@chiral mesoporous silica core–shell nanoparticles with unique optical properties. J Am Chem Soc, 2013, 135: 9659–9664
22 Han B, Zhu Z, Li Z, *et al.* Conformation modulated optical activity enhancement in chiral cysteine and Au nanorod assemblies. J Am Chem Soc, 2014, 136: 16104–16107
23 Li Z, Zhu Z, Liu W, *et al.* Reversible plasmonic circular dichroism of Au nanorod and DNA assemblies. J Am Chem Soc, 2012, 134: 3322–3325
24 Zhou Y, Yang M, Sun K, *et al.* Similar topological origin of chiral centers in organic and nanoscale inorganic structures: effect of stabilizer chirality on optical isomerism and growth of CdTe nanocrystals. J Am Chem Soc, 2010, 132: 6006–6013
25 Li J, Hu J, Ma C, *et al.* Uptake, translocation and physiological effects of magnetic iron oxide (γ-Fe_2O_3) nanoparticles in corn (Zea mays L.). Chemosphere, 2016, 159: 326–334
26 Zhou Y, Zhu Z, Huang W, *et al.* Optical coupling between chiral biomolecules and semiconductor nanoparticles: size-dependent circular dichroism absorption. Angew Chem Int Ed, 2011, 50: 11456–11459
27 Mallick S, Sharma S, Banerjee M, *et al.* Iodine-stabilized Cu nanoparticle chitosan composite for antibacterial applications. ACS Appl Mater Interfaces, 2012, 4: 1313–1323
28 Iconaru SL, Prodan AM, Le Coustumer P, *et al.* Synthesis and antibacterial and antibiofilm activity of iron oxide glycerol nanoparticles obtained by coprecipitation method. J Chem, 2013, 2013: 1–6
29 Li C, Wang X, Chen F, *et al.* The antifungal activity of graphene oxide–silver nanocomposites. Biomaterials, 2013, 34: 3882–3890
30 Yang L, Kuang H, Liu Y, *et al.* Mechanism of enhanced antibacterial activity of ultra-fine ZnO in phosphate buffer solution with various organic acids. Environ Pollut, 2016, 218: 863–869
31 Harifi T, Montazer M. *In situ* synthesis of iron oxide nanoparticles on polyester fabric utilizing color, magnetic, antibacterial and sono-Fenton catalytic properties. J Mater Chem B, 2014, 2: 272–282
32 Zeng T, Zhang X, Ma Y, *et al.* A novel Fe_3O_4–graphene–Au multifunctional nanocomposite: green synthesis and catalytic application. J Mater Chem, 2012, 22: 18658–18663
33 Cai A, Sun Y, Du L, *et al.* Hierarchical Ag_2O–ZnO–Fe_3O_4 composites with enhanced visible-light photocatalytic activity. J Alloys Compd, 2015, 644: 334–340
34 Fan X, Jiao G, Zhao W, *et al.* Magnetic Fe_3O_4–graphene composites as targeted drug nanocarriers for pH-activated release. Nanoscale, 2013, 5: 1143–1152
35 Roatti B, Perazzolli M, Gessler C, *et al.* Abiotic stresses affect *Trichoderma harzianum* T39-induced resistance to downy mildew in grapevine. Phytopathology, 2013, 103: 1227–1234
36 Cohen Y, Reuveni M, Baider A. Local and systemic activity of BABA (DL-3-aminobutyric acid) against *Plasmopara viticola* in grapevines. Eur J Plant Pathol, 1999, 105: 351–361

37 Boso S, Kassemeyer HH. Different susceptibility of European grapevine cultivars for downy mildew. Vitis, 2008, 47: 39-49
38 Perazzolli M, Dagostin S, Ferrari A, *et al.* Induction of systemic resistance against *Plasmopara viticola* in grapevine by *Trichoderma harzianum* T39 and benzothiadiazole. Biol Control, 2008, 47: 228–234
39 Luo K, Mu Y, Wang P, *et al.* Effect of oxidation degree on the synthesis and adsorption property of magnetite/graphene nanocomposites. Appl Surface Sci, 2015, 359: 188–195
40 Dai K, Lu L, Liu Q, *et al.* Sonication assisted preparation of graphene oxide/graphitic-C_3N_4 nanosheet hybrid with reinforced photocurrent for photocatalyst applications. Dalton Trans, 2014, 43: 6295–6299
41 Chen S, Zhu J, Wu X, *et al.* Graphene oxide–MnO_2 nanocomposites for supercapacitors. ACS Nano, 2010, 4: 2822–2830
42 Xue W, Zhao R, Du X, *et al.* Graphene–Fe_3O_4 micro–nano scaled hybrid spheres: synthesis and synergistic electromagnetic effect. Mater Res Bull, 2014, 50: 285–291
43 Alwarappan S, Erdem A, Liu C, *et al.* Probing the electrochemical properties of graphene nanosheets for biosensing applications. J Phys Chem C, 2009, 113: 8853–8857
44 Kiefer B, Riemann M, Büche C, *et al.* The host guides morphogenesis and stomatal targeting in the grapevine pathogen *Plasmopara viticola*. Planta, 2002, 215: 387–393
45 Kang S, Mauter MS, Elimelech M. Physicochemical determinants of multiwalled carbon nanotube bacterial cytotoxicity. Environ Sci Technol, 2008, 42: 7528–7534
46 Zhao S, Wang Q, Zhao Y, *et al.* Toxicity and translocation of graphene oxide in *Arabidopsis thaliana*. Environ Toxicol Pharmacol, 2015, 39: 145–156

Acknowledgments This work was supported by the National Natural Science Foundation of China (31501680 and 21277055), the Natural Science Foundation of Hebei Province (C2014407061 and C2014407008), and PhD Research Startup Foundation of Hebei Normal University of Science and Technology (2013YB005).

Author contributions Wang X conceived the project and wrote the manuscript. Cai A performed the synthesis and characterization of GO-Fe_3O_4. Jing D did all the bioassay experiments with the help of Wen X and Qi H. Yuan H supervised the project. All authors have given approval to the final version of the manuscript.

Conflict of interest The authors declare that they have no conflict of interest.

Supplementary information Supplementary data are available in the online version of the paper.

Xiuping Wang received her PhD degree in pesticide science from Huazhong Agriculture University in 2012. Now she is a lecturer at the College of Life Science and Technology, Hebei Normal University of Science and Technology. Her current research interests are in the intersection between plant protection and material science.

Hong Yuan received his PhD degree in analytical chemistry from the College of Chemistry and Molecular Sciences, Wuhan University, Wuhan, China, in 2003. Currently, he is a professor at the College of Chemistry, Central China Normal University. His research interests include the application of nanomaterials in environmental chemistry.

氧化石墨烯-四氧化三铁复合纳米材料对葡萄霜霉病杀菌活性的研究

王秀平[1], 蔡爱军[1], 温晓蕾[1], 静大鹏[1], 齐慧霞[1], 原弘[2*]

摘要 葡萄霜霉病由葡萄霜霉菌引起, 是一种广泛存在的葡萄病害, 严重威胁葡萄的田间正常生长. 虽然化学杀菌剂能有效控制病害, 但是容易导致病菌产生抗药性. 本文研究发现氧化石墨烯-四氧化三铁复合纳米材料可以有效地抑制葡萄霜霉菌的孢子萌发并控制霜霉病的发展. 试验结果表明, 50 μg mL^{-1}的氧化石墨烯-四氧化三铁复合纳米材料对葡萄霜霉病具有保护作用和杀菌效果. 田间试验结果表明, 250 μg mL^{-1}氧化石墨烯-四氧化三铁复合纳米材料可以显著降低葡萄霜霉病的病情指数, 具有较好的治疗作用. 高剂量(1000 μg mL^{-1})的氧化石墨烯-四氧化三铁复合纳米材料对葡萄叶片没有表现出明显的毒性. 本研究结果表明氧化石墨烯-四氧化三铁复合纳米材料有望成为防治葡萄霜霉病的一种新方法.